International Journal of Refrigeration 179 (2025) 420–431

Contents lists available at ScienceDirect

International Journal of Refrigeration

journal homepage: www.elsevier.com/locate/ijrefrig

INSTITUT INTERNATIONAL DU FROID
INTERNATIONAL INSTITUTE OF REFRIGERATION

Optimizing thermophysical properties of non-Newtonian nano-refrigerants for refrigeration systems using machine learning approaches

Mohammad Akbari [a,b], Seyed Amin Bagherzadeh [a,b], Mohammd Hossein Razavi Dehkordi [a,b], Alireza Naghsh [c], Noushin Azimy [d], Hamidreza Azimy [a,*]

[a] Department of Mechanical Engineering, Najafabad Branch, Islamic Azad University, Najafabad, Iran
[b] Aerospace and Energy Conversion Research Center, Najafabad Branch, Islamic Azad University, Najafabad, Iran
[c] Department of Electrical Engineering, Najafabad Branch, Islamic Azad University, Najafabad, Iran
[d] Department of Mechanical Engineering, Engineering Faculty, Shahid Chamran University of Ahvaz, Ahvaz, Iran

ARTICLE INFO

Keywords:
Thermophysical properties
Magnetocaloric refrigeration
Non-Newtonian nano-refrigerants
Heat transfer enhancement
Cooling systems
Optimization

ABSTRACT

The thermophysical properties of non-Newtonian superparamagnetic nano-refrigerants play a pivotal role in enhancing the efficiency of advanced cooling and next-generation refrigeration systems. The scope of this study includes the prediction and optimization of thermal conductivity and viscosity of cobalt ferrite ($CoFe_2O_4$)-based nanofluids over a range of temperatures and concentrations, targeting practical use in refrigeration system design. This study introduces a machine learning framework designed to predict and optimize the thermophysical properties of cobalt ferrite ($CoFe_2O_4$)-based superparamagnetic nano-refrigerants, with a focus on applications in refrigeration and heat transfer systems. By leveraging the capabilities of Radial Basis Function Networks (RBFNs), particularly a Generalized Regression Neural Network (GRNN), the model captures the relationships between critical input parameters such as temperature and nano-refrigerant concentration and key thermophysical outputs, including thermal conductivity and viscosity. To further enhance the framework, Particle Swarm Optimization (PSO) is integrated for inverse modeling, enabling the identification of optimal decision variables that balance thermal performance and magnetocaloric nano-refrigerant flow behavior. Unlike previous studies that rely primarily on empirical correlations or conventional simulations, this work introduces a hybrid machine learning–optimization framework that enables both predictive modeling and inverse design of thermally responsive nanofluids. The results reveal that increasing temperature significantly improves thermal conductivity, with an increase of 21.13 % at 50 °C, while viscosity rises by up to 61.38 % depending on nanoparticle loading at 50 °C. The model identifies an optimal mass fraction of ~0.3092 % at 50 °C, which achieves the best trade-off between heat transfer enhancement and acceptable flow behavior. Importantly, the proposed framework incorporates physical consistency checks and experimental constraints, ensuring robust and reliable predictions. These results validate the effectiveness of the integrated framework in addressing the challenges of thermophysical modeling for advanced cooling fluids. This work not only advances the understanding of non-Newtonian superparamagnetic nano-refrigerants but also demonstrates the transformative potential of combining neural networks with optimization techniques for data-driven modeling in refrigeration and heat transfer applications. The findings offer valuable insights for the development of next-generation cooling systems with improved efficiency and performance.

1. Introduction

One of the most effective parameters on thermal management at various industries is the working fluid type in a boiling, cooling, heating, ventilation, evaporation and other process cycle (Qun et al., 2024; Li et al., 2025; Al-Rbaihat et al., 2023). The conventional working fluids such as engine oil, water, and ethylene glycol have not a substantial thermal conductivity and heat transfer rate. On the other hand, solid metals have significant thermal conductivity and heat transfer rate; therefore, addition of solid metals with nano-dimensions to the conventional base fluids that named nanofluid leads to the thermal conductivity and heat transfer enhancement of the working fluid (Vaferi et al., 2014). In last decades, researchers have studied the thermal

* Corresponding author.
E-mail address: hamidrezaazimy@gmail.com (H. Azimy).

https://doi.org/10.1016/j.ijrefrig.2025.08.016
Received 21 March 2025; Received in revised form 10 August 2025; Accepted 14 August 2025
Available online 15 August 2025

Nomenclature

φ (x)	Gaussian function
φ_1 & φ_2	Constant
h	Convection heat transfer coefficient, (W/m^2.K)
T	Temperature (°C)
k	Thermal conductivity coefficient, (W/m.K)
μ	Viscosity (mPa.S)
R	Regression coefficient

Abbreviation

NPs	Nanoparticles
BF	Base Fluid
GRNN	Generalized Regression Neural Network
PSO	Particle Swarm Optimization
RBFN	Radial Basis Function Network
ANN	Artificial Neural Network
RSM	Response Surface Method
RT	Range of temperature
RC	Range of concentration
EG	Ethylene Glycol
FFNN	Feed-Forward Neural Network
p	Position
w	Water

Greek symbols

ρ	Density, (kg/m^3)
φ	Mass fraction, (%)

Subscripts

i	Initial

behavior, flow characteristics, CFD methods, and properties of various types of non-Newtonian and Newtonian fluids (Pourrajab et al., 2021; Pourrajab et al., 2020; Noghrehabadi et al., 2016). Many simulations and optimizations have been done to forecast the thermal behavior of fluids with different applications such as heat exchangers, batteries, combustion engines, and solar collectors (GAO et al., 2024; Azimy et al., 2024).

In order to prevent the high cost of experiments, researchers have taken notably more interest in soft computing techniques such as Artificial Neural Network (ANN), genetic algorithm, curve fitting, and fuzzy logic for estimating the thermal conductivity of nanofluids and developing a model for predicting nanofluids properties and rheological behavior (Azimy and Saffarian, 2023; DENG et al., 2024; Mandal et al., 2022; Wen et al., 2021). Here, a quick review of the research on ANN modeling of nanofluid thermal conductivity and their rheological behavior is done. Chu et al. (Seawram et al., 2022) compared the results of rheological behavior of TiO_2−MWCNT/5W40 hybrid nanofluid with regression-based methodologies. The influence of 0.05 %–1 % nanoparticles on the viscosity at 20–50 °C was measured. It was discovered that the maximum error was <5 % and that the viscosity ratio forecasting was satisfactory given that $R^2 = 0.999$. Ruhani et al. (Pourpasha et al., 2021) proposed a model for rheological behavior of a Newtonian hybrid nano-refrigerant with concentration of 0.1 %−1.5 % for Silica/EG-Water at temperature range of 25–50 °C in the shear rate of 24.48 s^{-1} to 73.44 s^{-1}. The graph indicates that the highest marginal deviation values are equal to 1.37 % that is acceptable for experimental correlation. The proportion of viscosity loss from the lowest temperature to the highest temperature at the highest volume concentration is 89 %. Yan et al. (Chu et al., 2021) studied the rheological behavior of TiO_2−MWCNTs (80–20 Vol %)/Ethylene glycol hybrid nano-refrigerant at temperature range of 25–55 °C. Based on the results, addition of nanoparticles has not changed its Newtonian behavior. Also, by enhancing the particles volume fraction and reducing the temperature, the dynamic viscosity improved. Safaei et al. (Ruhani et al., 2019) evaluated the thermal behavior of titanium oxide and zinc oxide nanoparticles in ethylene glycol based fluid utilizing ANN and Curve fitting and the results compared with experimental data. The outcomes have an acceptable agreement with ANN results that indicate ANN has capability to forecast the thermal characteristics of the nanofluid. Also, the ANN results are more accurate rather curve fitting methodology. Melaibari et al. (Yan et al., 2020) employed the Response Surface Methodology (RSM) and ANN to predict the rheological behavior of copper oxide and graphene oxide nanoparticles dispersed in water and ethylene glycol. Results indicate that the nano-refrigerant has Newtonian behavior at 0.1, 0.2, and 0.4 % volume fraction, however, in higher volume fraction, the nano-refrigerant shows non-Newtonian behavior. The comparison between both RSM and ANN methods shows that R-squared for RSM and ANN is 0.944 and 0.995, respectively that prove the superiority of ANN method. Hemmat Esfe et al. (Safaei et al., 2019) investigated the rheological behavior of Mg/motor oil nanofluid. The viscosity outcomes show that all of the samples demonstrate shear-thinning characteristics. In order to model the experimental findings, the ANN is utilized. Sepehrnia et al. (Melaibari et al., 2021) optimized and evaluated the dynamic viscosity and rheological characteristics of SiO_2−MWCNT dispersed in 5W30 engine oil at various volume concentration, shear rate, and temperature. A three-variable correlation proposed for relative viscosity of hybrid nanofluid. When using a constant shear rate of 800 rpm, it was found that the dynamic viscosity sensitivity enhances as the nanofluid concentration and temperature enhances. Hemmat Esfe et al. (Esfe et al., 2017) investigated the dynamic viscosity of MWCNT-MgO nanoparticles dispersed in SAE40 engine oil at various temperature, shear rate, solid volume fraction and validated the results utilizing ANN with the Levenberg–Marquardt learning algorithm. The findings demonstrate that the best ANN for predicting viscosity has the least mean square error (MSE) and the highest regression coefficient R near to 1. Azimy et al. (Sepehrnia et al., 2024) evaluated the thermal characteristics of a heat exchanger including nanofluid under ultrasonic wave power variation and validated the experimental results with ANN. They used backpropagation as a training methodology for this network. They found “trainbr” training algorithm and an ANN with 15 hidden neurons as a perfect combination for their research.

Sepehrnia et al. (Esfe et al., 2023) investigated the rheological characteristics of a MoO_3-GO-MWCNTs nanoparticles dispersed in 5W30 engine oil at various condition experimentally and using ANN. Dynamic viscosity was predicted using a three-variable correlation, which had a respectable level of accuracy ($R = 0.9931$). Additionally, a model with an unusually high level of accuracy ($R^2 = 0.999709$) was created for calculating the viscosity of the hybrid nano-lubricants by optimizing the GP-based ANFIS structure. Kamsuwan et al. (Azimy et al., 2023) forecasted an ANN model for nanofluids behavior in heat exchanger. Results reveal that in compare with classical models, the ANN combination can forecast nanofluid behavior and has superior accuracy. Hatamleh et al. (Sepehrnia et al., 2023) evaluated the thermos-electrical performance of the solar cooling system’s panel in presence of nanofluids by utilizing ANN. Based on the results, utilizing nanofluid instead of typical working fluids improves thermos-electrical efficiency of the solar cooling system. The solver’s ability to do precise and accurate computations is demonstrated by the mean square error up to 10–12 for a hybrid nanofluid flow over a shrinking/stretching surface in Shoaib et al. (Kamsuwan et al., 2023) research. Ünvar et al. (Hatamleh et al., 2023) experimentally analyzed the power and performance of the solar collector including nanofluid and developed an

ANN model. Their findings indicate utilizing TiO_2 and Al_2O_3 nanofluid improve the efficiency and power of the heat pipe solar collector. The study also revealed that the created ANN model is capable of predicting efficiency and power values with variation rates under 0.48 %. Table 1 summarizes previous research on various coolant and nanofluids' thermal conductivity and viscosity.

Numerous studies have been conducted to date to examine the significant function and thermal behavior of various nano-refrigerants used in diverse applications using ANN method (El Jery et al., 2023a,b; Khosravi et al., 2023; Kim et al., 2021; Kumar et al., 2023; Sun et al., 2021). In addition, studies on the usage of $CoFe_2O_4$ colloidal NPs cluster particles have been conducted experimentally (Abbasian et al., 2024). However, a comprehensive numerical framework for modeling the thermophysical properties (thermal conductivity and viscosity) of $CoFe_2O_4$-based superparamagnetic nano-refrigerants using ANN has not yet been reported. In particular, no previous work has addressed the behavior of these superparamagnetic nanofluids using a machine learning approach combined with optimization techniques. The main objective of this study is to develop a predictive and inverse design model using a Generalized Regression Neural Network and Particle Swarm Optimization to estimate and optimize key thermophysical parameters of $CoFe_2O_4$ nano-refrigerants under varying temperatures and concentrations. The novelty of this work lies in applying a hybrid neural network–optimization framework to analyze the thermophysical behavior of superparamagnetic nanofluids and to explore their potential application in next-generation cooling systems, particularly as magnetocaloric working fluids.

2. Materials and methods

The experimental data for thermal conductivity and viscosity were obtained from the published study by Abbasian et al. (Abbasian et al., 2024), where full experimental procedures are documented. In that work, the cobalt ferrite colloidal nanoparticles were synthesized and dispersed in an ethylene glycol (EG)-water (50:50) coolant base fluid using a 2-step method at varying mass concentrations: 0.05 %, 0.1 %, 0.2 %, 0.4 %, and 0.8 %. In addition, the nanoparticle mass fraction was limited to a maximum of 0.8 % to maintain suspension stability, as higher concentrations have been shown to increase the risk of nanoparticle agglomeration and sedimentation. This value represents an optimal balance between enhancing thermophysical properties and ensuring long-term stability, consistent with previous experimental findings (Abbasian et al., 2024). Initially, the nanoparticles were added to the base fluid at a specific mass percentage and stirred with a magnetic stirrer for sufficient time until a stable colloidal mixture was achieved. Ultrasonic waves were then applied for 20 min to each sample to prevent agglomerate and ensure suspension stability of the nanoparticles. To maintain the stability of the magnetocaloric nano-refrigerant, the experiment was conducted within a temperature range of 10 to 50 °C. Thermal conductivity and viscosity parameters were measured in different temperatures and concentrations. So, in this study the optimization of these thermophysical properties was performed using multi-objective machine learning techniques to balance the parameters, particularly important in non-Newtonian behavior.

In addition, the input variables used in this study, temperature and nanoparticle mass fraction, were selected based on both fundamental physical understanding and extensive literature evidence. Temperature is known to influence Brownian motion, molecular collisions, and fluid structure, thereby affecting both thermal conductivity and viscosity. Similarly, nanoparticle concentration (mass fraction) alters particle–fluid interactions, clustering, and effective heat transfer pathways. These two parameters have consistently been identified in prior experimental and modeling studies as dominant factors controlling the thermophysical behavior of nanofluids.

2.1. The machine learning method

The adoption of Machine Learning (specifically the Generalized Regression Neural Network, GRNN) and Particle Swarm Optimization (PSO) in this study was motivated by the nonlinear, multivariable nature of nano-refrigerant thermophysical properties. Conventional empirical correlations often struggle to represent the coupled effects of temperature, concentration, and non-Newtonian behavior. GRNN offers accurate predictions from limited datasets, while PSO efficiently identifies optimal trade-offs between thermal conductivity and viscosity, two properties that often have conflicting design requirements. This combined framework provides a rapid, data-driven decision-making tool for optimizing next-generation refrigeration systems. To implement the GRNN component of our framework, we employed a Radial Basis Function Network (RBFN) structure, which forms the underlying architecture of GRNN models. Radial Basis Function Networks (RBFNs) represent a specialized class of artificial neural network architectures with applications spanning various machine learning tasks, including regression and classification. RBFNs derive their name from the utilization of with radial basis functions (RBFs) within their hidden layer, which distinguish them from conventional feedforward neural networks. This feature enables them to model intricate non-linear relationships in data effectively RBFNs comprise three primary layers: an input layer, a hidden layer with radial basis functions, and an output layer. The input layer accommodates features, whether continuous or categorical, typically subjected to normalization. The heart of RBFNs is in the hidden layer, where each neuron is associated with RBF. The RBF computes its activation by assessing the Euclidean distance between the input data and a designated center point. The Gaussian function is the most frequently employed RBF, offering adaptability via its spread parameter. The Gaussian function can be defined as follows:

$$\varphi(x) = exp\left[-\frac{\| x - c\|^2}{2\sigma^2}\right] \quad (1)$$

Here, x is the input data vector, c is the center point of the RBF, and σ is a parameter that controls the spread or width of the RBF's response. The output layer typically consists of a single neuron. The output of the network is the weighted sum of the activations of the RBF neurons in the hidden layer. This weighted sum serves as the predicted continuous output value. The architecture of the RBFN is illustrated in Fig. 1.

Training RBFNs involves the determination of RBF centers and spread parameters. Various techniques can be employed, such as k-means clustering or gradient descent, to optimize these parameters with respect to the training data. This phase is pivotal in enabling RBFNs to capture the underlying data distribution effectively.

RBFNs find extensive utility across a spectrum of machine learning tasks. In regression tasks, a single output neuron in the RBFN computes a weighted sum of hidden layer activations, yielding continuous predictions. RBFNs have exhibited prowess in function approximation, time series forecasting, and modeling complex non-linear data relationships.

In this paper, a special type of RBFNs is employed, namely the Generalized Regression Neural Network (GRNN). The GRNN is a type of artificial neural network that is primarily used for regression tasks. The key characteristic of a GRNN is the hidden layer consists of a set of RBF activation functions. GRNNs are known for their ability to approximate complex non-linear relationships in data, making them suitable for a wide range of regression tasks. GRNN offers several advantages over traditional backpropagation-based networks, including faster training due to its one-pass learning mechanism, eliminating the need for iterative optimization. Unlike backpropagation networks, which can get stuck in local minima, GRNN provides a direct solution based on kernel smoothing, ensuring stable performance. It excels in nonlinear regression tasks by leveraging smooth interpolation between data points and handles noisy data effectively due to its averaging nature. Additionally, GRNN requires fewer hyperparameters to tune compared to deep

Table 1
A comprehensive synopsis of previous research on the thermal conductivity and viscosity of various nanofluids.

Ref	BF	NPs	RT	RC	Results
(Shoaib et al., 2023)	R1123 + R32 refrigerant mixture	None (pure refrigerant mixture)	250.64–312.61 K (liquid), 323.35–382.88 K (vapor)	R1123/R32 mass fraction: 0.428/0.572 (liquid), 0.425/0.575 (vapor)	Viscosity measured in both phases; average absolute deviation (AAD) = 3.63 % (liquid), 2.45 % (vapor) vs. ECS model; Grunberg–Nissan and Wilke correlations used with AADs of 1.33 % and 3.69 %, respectively.
(Ünvar et al., 2023)	R1336mzz(E) (trans-hexafluoro-2-butene)	None	313–453 (liquid, vapor, supercritical)	Pure refrigerant	Thermal conductivity measured using transient hot-wire method; saturated and supercritical data modeled; uncertainty: 1.94 %–2.01 %; compared to R1336mzz (Z).
(Mondal et al., 2020)	R1336mzz(E)	None	314–453 (liquid, vapor, supercritical)	Pure refrigerant	Viscosity measured via tandem capillary tubes. AAD vs. ECS model: 5.04 % (liquid), 22.19 % (vapor), 11.88 % (supercritical); uncertainty: ~2.3 %; correlations for saturated conditions developed.
(Mondal et al., 2021)	3,3,4,4,5,5-HFCPE (1H,2H-hexafluorocyclopentene)	None	Viscosity: 332–514 K; Conductivity: 333–473 K (liquid, vapor)	Pure refrigerant	Kinematic viscosity and thermal conductivity measured using tandem capillary tubes and transient hot-wire. Uncertainty: ~2.2–3.5 %; simple correlations for saturated conditions developed.
(D. Mondal et al., 2022)	Water (80 %) + Ethylene Glycol (20 %)	MWCNT + Al_2O_3 (Hybrid)	Not specified (varied)	Nanoparticle volume fraction (variable)	MLPNN used for viscosity prediction; PSO yielded highest accuracy ($R = 0.99995$, MSE = 0.00105); VF had strongest effect on viscosity via sensitivity analysis.
(D. Mondal et al., 2022)	Water	GNP + Fe_2O_3 (Hybrid)	293–328 K (20–55 °C)	Variable GNP:Fe_2O_3 ratios	ANN and RSM used to model thermal conductivity, viscosity, and electrical conductivity; ANN outperformed RSM; temperature ↑ → TC↑, EC↑, viscosity↓; higher GNP ratio increased TC but lowered EC and viscosity.
(Ru et al., 2025)	Deionized Water	CeO_2-MWCNT (Hybrid)	293–323 K (20–50 °C)	Solid volume fractions (0.007 ≤ SVF ≤ 0.112 %)	Thermal conductivity measured via hot-wire; max ThC enhancement at 0.112 % SVF and 50 °C; ANN model ($R^2 = 0.9918$, max deviation = 0.438 %); longer sonication improved stability and ThC.
(Borode et al., 2024)	Ethylene Glycol	Flamboyant Tree Bark (FTB) bio-NPs	293–343 K (20–70 °C)	0.2–1.0 vol %	Bio-based nanofluid tested; max viscosity ↑75 %, pH ↑26 %, EC ↑104 % at 1.0 % and 70 °C; all properties increased with concentration; viscosity and pH decreased with T, EC increased with T.
(Alqaed et al., 2024)	Water	MgO + ZnO + MWCNT (Ternary)	288–333 K (15–60 °C)	0.10 vol %	EC ↑907.4 %, viscosity ↑34 %; viscosity ↓ with temp.; ternary NF outperformed single NFs in stability and conductivity.
(Awua et al., 2024)	Ethylene glycol + water (60:40)	Al_2O_3 + TiO_2 + SiO_2 (Ternary)	303–343 K (30–70 °C)	0.05 - 0.3 vol %	Thermal conductivity ↑ 9 % at 0.3 vol %. (70 °C); 4.8 % ↑ at 0.05 vol %. (70 °C); viscosity decreases with temperature; higher concentration improves heat transfer
(Momin et al., 2025)	Ethylene glycol + water (60:40)	GNP + CNC (Hybrid)	303 – 353 K (30–80 °C)	0.01 – 0.2 vol %	TC ↑ with temp.; max stability and UV–Vis absorbance at 0.1–0.2 %; thermal resilience onset at 130–150 °C; ANN model (R^2 = 99.99 %) predicted TC with high accuracy
(Ramadhan et al., 2023)	Ethylene glycol + water (80:20)	CuO	288 – 323 K (15–50 °C)		Viscosity modeled via RSM; Quartic model selected as best fit; optimal viscosity: 8.565 mPa.s at 298.45 K, 0.05 % SVF, 26.66 s^{-1} SR
(Hasan et al., 2025)	Ethylene glycol + water	Al_2O_3 + ZnO + TiO_2 (nanocomposite)	293 – 453 K (20–180 °C)	0.3, 0.6, 0.9 vol %	TC, SHC, and viscosity improved with nanocomposite loading; max TC at 0.9 % vol; validated via regression analysis and mathematical models
(Hemmat Esfe et al., 2024)	Deionized water	Fe_3O_4/TiO_2, Fe_3O_4/MgO, Fe_3O_4/ZnO (Hybrid MHFs)	283 – 323 K (10–50 °C)	0.3 vol %; HMR: 80:20, 60:40, 40:60	Max TC ↑31.28 % for Fe_3O_4/ZnO at 50 °C (0.793 W/m·K); EC ↑972.93 % for Fe_3O_4/TiO_2 (18 nm); viscosity ↓ with T; best stability and performance at HMR 80:20
(Karakaş et al., 2022)	Various (water, EG, oils, etc.)	Metal oxides (e.g., Al_2O_3, ZnO, TiO_2, CuO, etc.)			TC ↑ depends on T, conc., NP size, shape, alignment, surfactants, sonication, field effects; electric/magnetic fields enhance TC; transient hot wire widely used; green NFs recommended

(*continued on next page*)

Table 1 (*continued*)

Ref	BF	NPs	RT	RC	Results
(Adogbeji et al., 2025)	Deionized water	Graphene nanoplatelets (GNP) + γ-Al_2O_3	288– 313 K (15–40 °C)	0.1 – 04 vol %	At 0.4 %: μ ↑21.74 %, λ ↑17.82 %, σ ↑393.36 % at 313 K; ANFIS model (R^2 > 0.99) predicted μ, λ, σ; optimal performance at 0.1–0.2 %
(Yasmin et al., 2023)	R-1132(E)	None	233–335 K (liquid), 333–373 K (vapor)	Pure refrigerant	Viscosity measured via tandem capillary tube; uncertainty: 2.24 % (liq.), 2.28 % (vap.); ECS and modified Residual Entropy Scaling models accurately predict viscosity
(Borode et al., 2023)	Low-GWP refrigerants (7 halogenated alkenes)			Pure refrigerant	Neural network model (5 input features) trained on 3404 datapoints; AARD = 0.389 %, max deviation = 6.074 %; outperformed REFPROP 10 and other correlations
(Tran et al., 2025)	Pure R1243zf; R32 + R1243zf; R32 + R1234yf	None	264.1–405.6 K	R32 mole fraction: 0.25, 0.50, 0.75	λ measured (liquid + vapor); uncertainty ≈ 2 %; ECS model deviation: −14–10 %; RES-CPA model matched ECS without extra binary interaction parameters
(Pierantozzi et al., 2023)	POE75 oil + R1234yf/ze(E)	None	303–348 K	Refrigerant mole fraction (variable)	Viscosity ↓ sharply with ↑ refrigerant solubility; Eyring-MTSM model best fit (max deviation: 2.57 %–1.87 %); R1234ze (E) ↓ viscosity more than R1234yf.

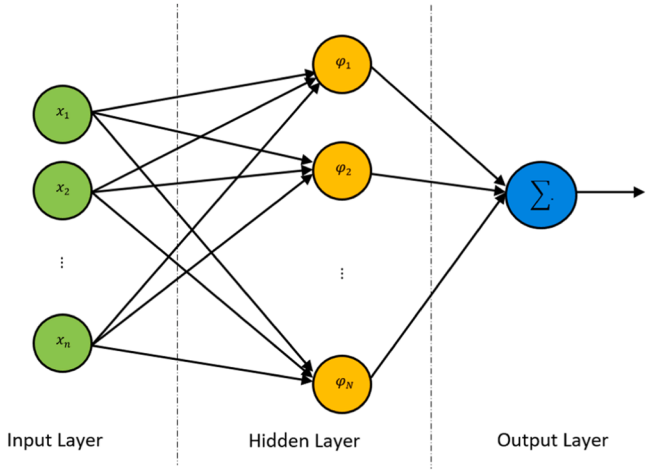

Fig. 1. The architecture of the RBFN.

learning models, making it simpler to implement while still maintaining strong approximation capabilities for continuous functions. These qualities make GRNN particularly useful in real-time applications and scenarios where rapid model deployment is essential. The flowchart for the RBFN is illustrated in Fig. 2.

2.2. The optimization method

Particle Swarm Optimization (PSO) is a computational method for solving optimization problems inspired by the social behavior of birds and fish. It involves a group of potential solutions, called particles, that move through the solution space, each adjusting its position based on its own experience (i.e., personal best) and the best experience of the swarm (i.e., global best). By iteratively updating their positions and velocities according to mathematical formulas, particles explore the search space collectively, allowing the swarm to converge towards optimal solutions. PSO is valued for its simplicity, efficiency, and versatility, making it applicable in various fields.

The PSO Algorithm contains the following Steps:

- Initialization:
  - Define the problem and the objective function to optimize.
  - Initialize a swarm of particles (i.e., candidate solutions) with random positions and velocities in the solution space. Each particle has an initial position and velocity: $p_i(0)$ and $v_i(0)$
  - Set parameters such as the number of particles, maximum iterations, and coefficients c_1 and c_2 for cognitive and social components.
- Evaluate Fitness:
  - Evaluate the fitness of each particle based on the objective function. The fitness value helps determine the quality of the particle's current position.
- Update Personal Best:
  - For each particle, compare its current fitness value with its personal best fitness value:
  - If the current fitness is better, update its personal best position: $p_{best,i} = p_i$ if $p_i < p_{best,i}$
- Update Global Best:
  - Identify the best position among all particles, known as the global best: $g_{best} = arg\ min_i\left(f\left(p_{best,i}\right)\right)$
- Update Velocities and Positions:
  - Update the velocity and position of each particle using the following equations:

$$v_i(t+1) = w\ .\ v_i(t) + c_1 \cdot r_1 \cdot \left(p_{best,i} - p_i(t)\right) + c_2 \cdot r_2 \cdot \left(g_{best} - p_i(t)\right) \quad (2)$$

$$p_i(t+1) = p_i(t) + v_i(t+1) \quad (3)$$

- Apply Boundary Conditions:
  - Check if the updated position of any particle exceeds the defined boundaries of the search space. If it does, apply boundary conditions (e.g., reflecting the particle back or resetting it within the bounds).
- Check Stopping Criteria:
  - Determine if the algorithm should terminate. This could be based on criteria such as a maximum number of iterations has been reached, the improvement in the global best position is below a certain threshold or a solution within acceptable fitness has been found.
- Repeat:
  - If the stopping criteria are not met, return to step 2 and repeat the process until termination conditions are satisfied.

In PSO, r_1 and r_2 are random coefficients used to introduce stochastic behavior into the velocity update equations of the particles. Each particle generates its own r_1 and r_2 values at each iteration, meaning the

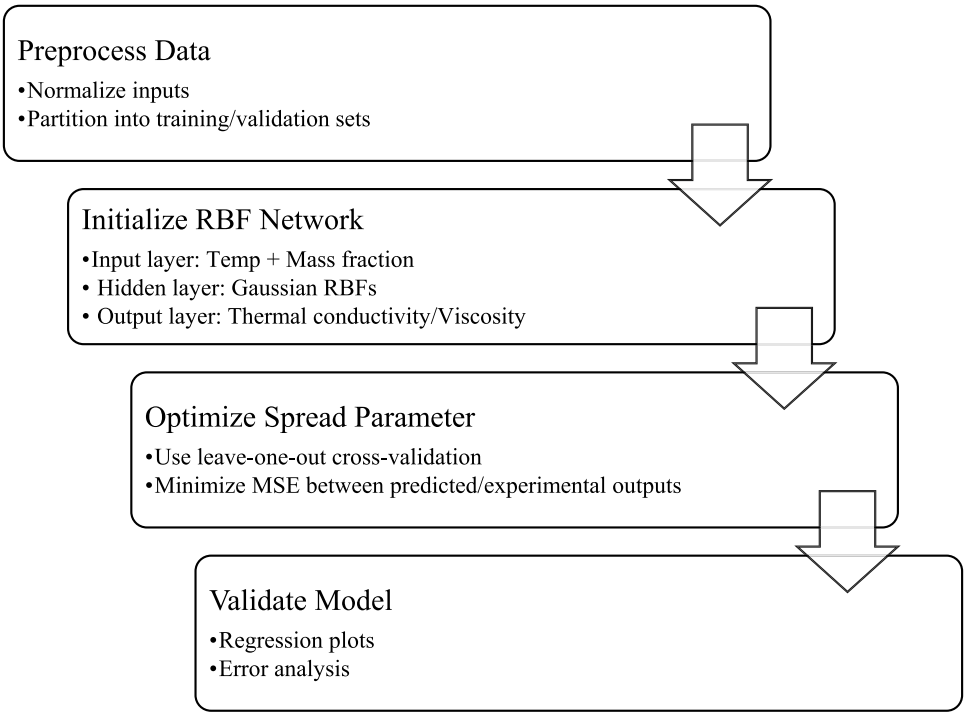

Fig. 2. The flowchart for the RBFN.

influence of personal and global bests on the particle's movement can vary with each update. The random nature introduced by r_1 and r_2 ensures that particles do not follow a deterministic path. Instead, they explore the solution space more broadly, which helps avoid local optima and promotes diversity within the swarm. This randomness allows particles to explore various areas of the search space, enabling them to escape from local optima and search for global solutions more effectively. The overall behavior of the PSO algorithm is inherently stochastic due to the random components. This randomness can lead to different outcomes in different runs of the algorithm, even with the same initial conditions and parameters. This variability is a double-edged sword; it can help in discovering diverse solutions but may also lead to inconsistency.

In this paper, the parameters c_1, c_2, and w are selected by the adaptive method presented in (Salins et al., 2024), as follows:

$$c_1 = \varphi_1 \, w \tag{4}$$

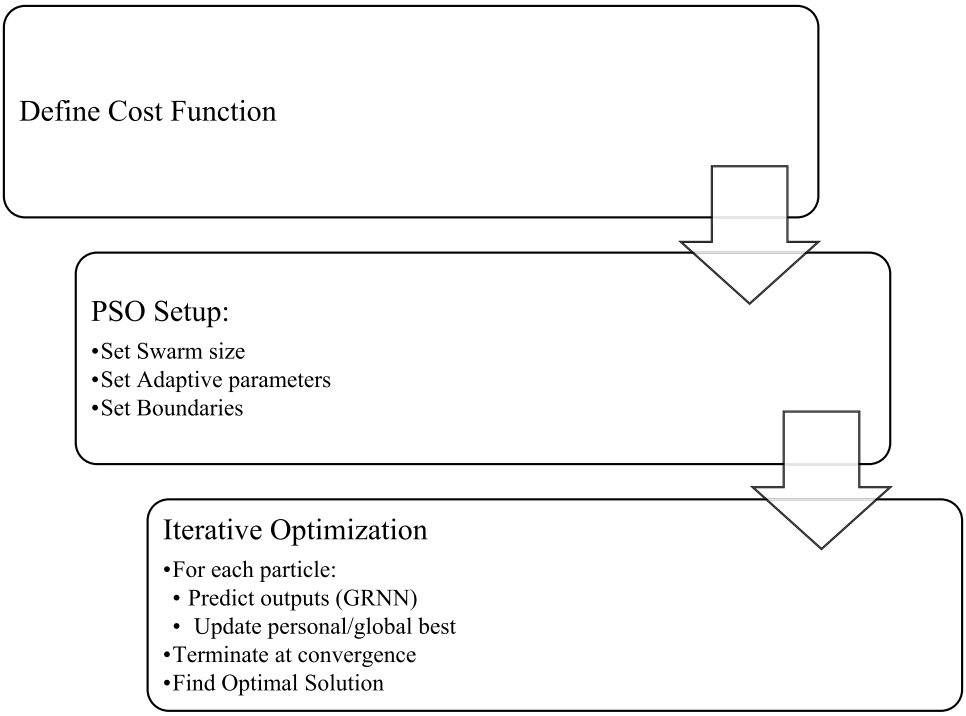

Fig. 3. The flowchart for the PSO.

$$c_2 = \varphi_2 \, w \tag{5}$$

$$w = \frac{2k}{\left|2 - (\varphi_1 + \varphi_2) - \sqrt{(\varphi_1 + \varphi_2)^2 - 4 * (\varphi_1 + \varphi_2)}\right|} \tag{6}$$

in which φ_1, φ_2, and k are constants.

The flowchart for the PSO is illustrated in Fig. 3.

3. Results

3.1. The GRNN results

In this section, the results of the GRNN applied to the studied problem is investigated. The inputs are the temperature and mass fraction of the nano-refrigerant. The outputs are the nano-refrigerant characteristics, namely the thermal conductivity and viscosity. 30 independent tests are conducted for dissimilar input pairs, while other conditions are maintained fixed (Table 2). Although limited studies have investigated the properties of superparamagnetic nanofluids, existing research consistently shows that the addition of nanoparticles to a base fluid generally leads to increases in both thermal conductivity and viscosity (Dehkordi et al., 2023; Eshgarf et al., 2023). For example, Puspitasari et al. (Puspitasari et al.) reported that adding $ZnFe_2O_4$ nanoparticles to polyester oil (POE) refrigeration lubricant enhanced thermal conductivity by up to 1.6 %. Similarly, Amani et al. (Amani et al., 2017) found that at 30 °C, increasing the volumetric concentration of $MnFe_2O_4$ nanoparticles from 0 to 3 % in water resulted in approximately a 12 % improvement in thermal conductivity. In the present study, at the same temperature (30 °C), increasing the mass concentration of $CoFe_2O_4$ nanoparticles from 0 to 0.8 % led to a 19.75 % enhancement in thermal conductivity, confirming the trends reported in prior studies. In terms of viscosity, Eshgarf et al. (Eshgarf et al., 2023) demonstrated that increasing the Fe_3O_4 nanoparticle concentration from 0 to 0.3 % by mass at 30 °C raised the viscosity by 6.66 %. In comparison, the present study observed an 84.5 % increase in viscosity upon nanoparticle addition, which supports the expected rheological behavior of nanofluids containing superparamagnetic particles.

The GRNN-PSO model also identified an optimal nano-refrigerant mass fraction of approximately 0.3092 % at 50 °C. This result aligns with the expected nonlinear behavior of magnetocaloric nanofluids, where thermal conductivity and viscosity are both sensitive to nanoparticle concentration and temperature. At low concentrations, superparamagnetic nanoparticles enhance thermal transport due to Brownian motion, liquid layering, and improved phonon interactions. However, beyond a certain threshold, increased viscosity and particle aggregation reduce the effectiveness of heat transfer, particularly in natural convection-dominated systems. At 50 °C, the viscosity of the base fluid decreases while nanoparticle motion increases, supporting enhanced conductivity up to an optimal limit. The identified optimum reflects this balance, where the benefits of nanoparticle addition are maximized before negative rheological effects become dominant.

After the training process, one can create a regression plot for the training dataset. A regression plot, often referred to as a scatterplot with a fitted regression line, is a graphical representation used in statistical analysis to visualize the relationship between two continuous variables. In this case, the horizontal axis represents the targets, while the vertical axis represents the numerical output of the GRNN. Each data point in the plot corresponds to a pair of values from these two variables, creating a cloud of points scattered across the graph. The key feature of a regression plot is the fitted regression line that best captures the trend within the data. This line is determined by the linear regression, which minimizes the sum of squared differences between the observed data points and the predicted values along the line. The regression plots for the viscosity and thermal conductivity are shown in Figs. 4 and 5.

The regression value, slope and intercept of the regression line convey crucial information about the relationship. The regression value indicates the goodness of fit of the regression model to the data. The

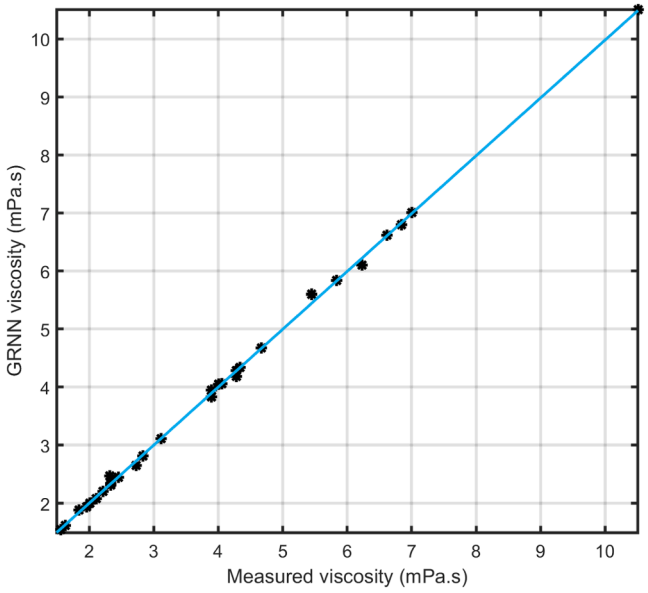

Fig. 4. The regression plots for the viscosity.

Table 2
The used experimental data as input and output parameters for Radial Basis Function Networks (Abbasian et al., 2024).

Input Parameters		Output Parameters		Input Parameters		Output Parameters	
Temperature (°C)	Mass fraction (%)	Thermal conductivity (W/m.K)	Viscosity (mPa.S)	Temperature (°C)	Mass fraction (%)	Thermal conductivity (W/m.K)	Viscosity (mPa.S)
10	0	0.318	5.45	30	0.20	0.375	3.89
10	0.05	0.349	5.84	30	0.40	0.379	4.06
10	0.10	0.357	6.23	30	0.80	0.388	4. 28
10	0.20	0.362	6.84	40	0	0.331	1.84
10	0.40	0.365	7.01	40	0.05	0.366	1.96
10	0.80	0.37	10.51	40	0.10	0.379	2.01
20	0	0.322	3.89	40	0.20	0.386	2.34
20	0.05	0.354	4.01	40	0.40	0.391	2.45
20	0.10	0.364	4.28	40	0.80	0.399	3.11
20	0.20	0.37	4.34	50	0	0.336	1.45
20	0.40	0.373	4.67	50	0.05	0.372	1.56
20	0.80	0.383	6.62	50	0.10	0.387	1.63
30	0	0.324	2.32	50	0.20	0.395	2.11
30	0.05	0.358	2.73	50	0.40	0.4	2.21
30	0.10	0.369	2.83	50	0.80	0.407	2.34

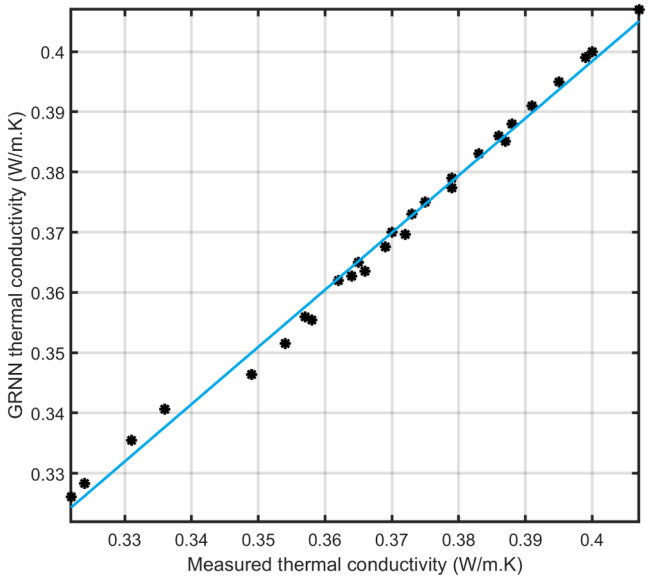

Fig. 5. The regression plots for the thermal conductivity.

slope, and intercept of the regression plot collectively characterize the relationship between the measured and predicted response. The regression value, slope and intercept of the regression lines are shown in Table 3. Based on the results, it can be observed that the GRNN is successfully applied to the studied problem, and the measured targets and numerical outputs are almost identical. For comparison, results of a conventional Feed-Forward Neural Network (FFNN) with 10 hidden neurons trained using the Levenberg–Marquardt algorithm is also reported in Table 3. As can be seen, the GRNN obtains better results in comparison with the FFNN.

To rigorously evaluate the GRNN's generalizability beyond the training data, two cross-validation approaches are employed: (1) Leave-One-Out Cross-Validation (LOOCV), where the model was iteratively trained on all data points except one (n-1) and tested on the excluded point, repeated for all 30 experimental cases; and (2) 5-Fold Cross-Validation, where the dataset was randomly partitioned into five equal subsets, with each subset serving as the test set while the remaining four were used for training. These methods comprehensively assess prediction stability across different data splits, with LOOCV providing maximal training data utilization (29/30 points per iteration) and 5-fold validation simulating real-world scenarios with limited data. The consistency between both methods presented in Table 4 confirms the model's robustness against overfitting.

The relative error between the measured targets and outputs predicted by the GRNN are shown in Figs. 6 and 7 for the viscosity and thermal conductivity, respectively. As can be seen, the error values are <8 % for the viscosity, and <1.5 % for the thermal conductivity.

The error histograms are shown in Figs. 8 and 9 for the viscosity and thermal conductivity, respectively. The error histogram is a graphical representation that displays the distribution of prediction errors made by the GRNN model. This histogram provides insights into the performance and behavior of the model by visualizing the discrepancies between the predicted values and the actual target values. As can be seen,

Table 3
The regression value, slope and intercept of the regression lines.

		Regression value	Slope	Intercept
GRNN	**Viscosity**	0.9996	0.9973	0.0098
	Thermal conductivity	0.9968	0.9492	0.0108
FFNN	**Viscosity**	0.9783	0.9814	0.0124
	Thermal conductivity	0.9752	0.9271	0.0195

Table 4
Cross-validation performance.

Property	LOOCV MSE	5-Fold MSE	LOOCV R^2	5-Fold R^2
Thermal conductivity	0.012	0.014	0.9965	0.9958
Viscosity	0.085	0.092	0.9989	0.9983

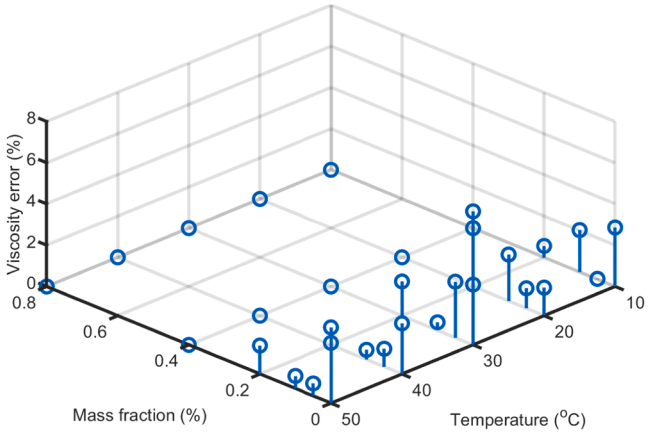

Fig. 6. The relative error between the measured targets and outputs predicted by the GRNN for the viscosity.

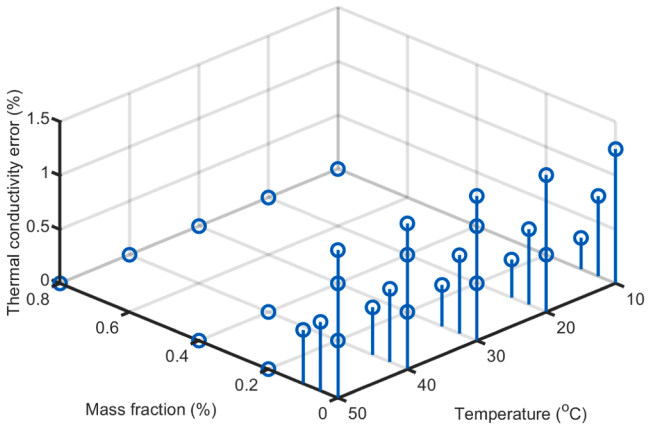

Fig. 7. The relative error between the measured targets and outputs predicted by the GRNN for the thermal conductivity.

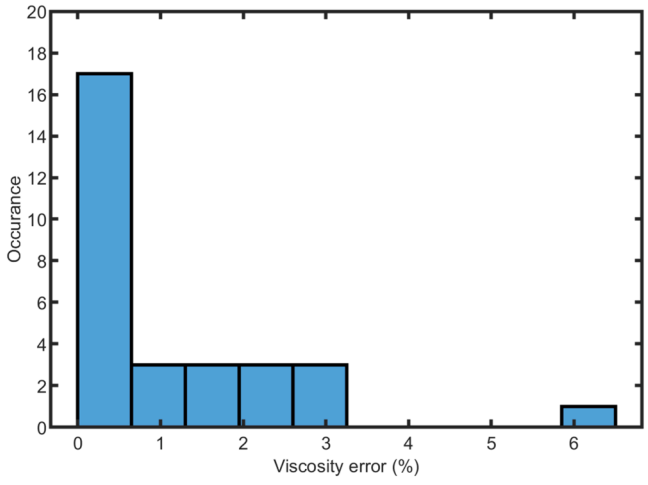

Fig. 8. The error histogram for the viscosity.

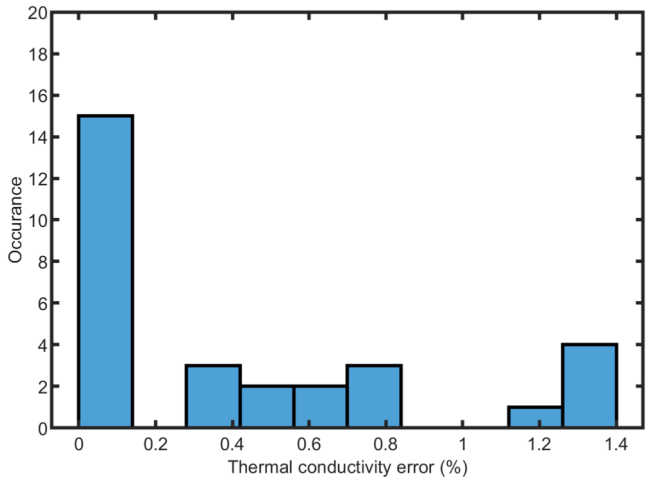

Fig. 9. The error histogram for the thermal conductivity.

the error is concentrated around 0, while some outliers can be seen with higher error values. Therefore, The GRNN has acceptable accuracy for the prediction of the viscosity and thermal conductivity.

Finally, one can the trained GRNN models to predict the viscosity and thermal conductivity for any desired temperature and mass fraction of the nano-refrigerant in the examined ranges. The results are shown in Figs. 10 and 11. In these plots, the asterisks show the experimental data, while the contour is the outputs predicted by the GRNN.

The results demonstrate that the models effectively capture and represent the underlying relationship between input variables and the corresponding outputs due to the following reasons:

- It can be seen that there is a close agreement between the model's predictions and the actual data points since the contours closely match the distribution of data points.
- The output contours generated by the model are smooth and continuous. This indicates that the model is able to interpolate between data points and provide predictions for input values that were not explicitly part of the training data.

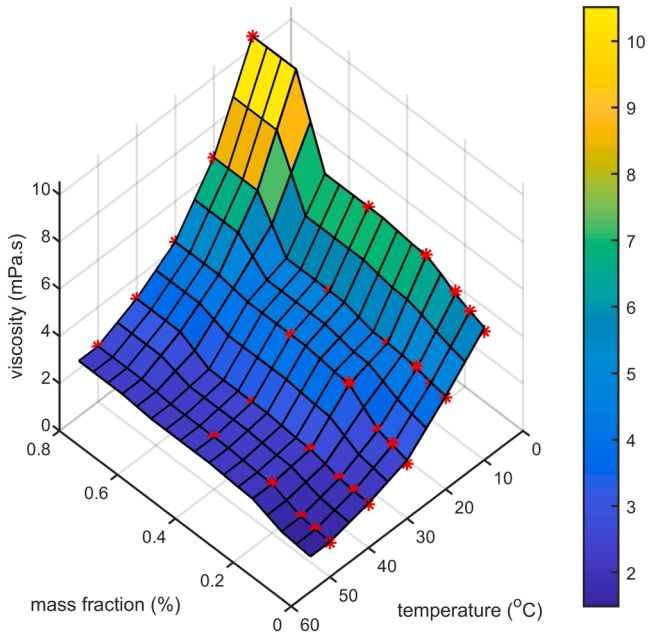

Fig. 10. The viscosity obtained by the GRNN in the examined range.

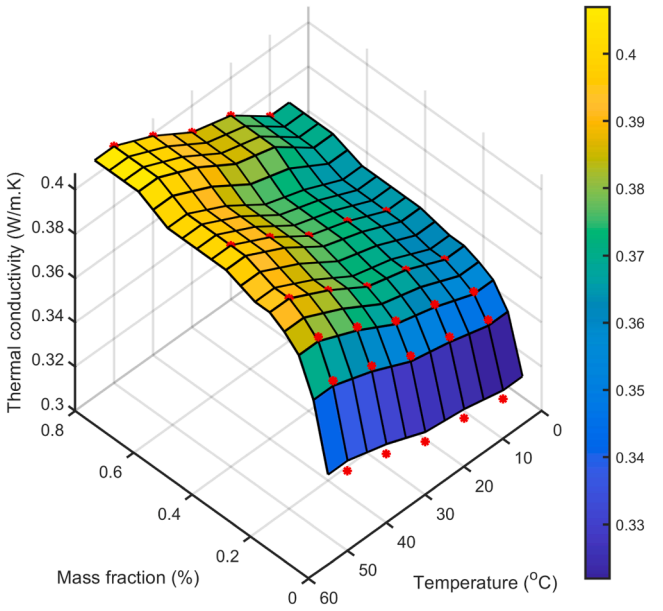

Fig. 11. The thermal conductivity obtained by the GRNN in the examined range.

- The contours should exhibit consistent patterns and trends that align with the underlying physical or scientific principles.
- The residuals are randomly scattered around zero, indicating that the model captures the main trends and patterns in the data.
- The fit is not only applicable to the training data but also extends to unseen data. In dealing with non-trained datasets, the model continues to provide accurate predictions, and the contours remain consistent.
- The quantitative metrics, such as regression values and relative error, indicate acceptable fits.

In summary, it can be seen that the GRNN models accurately represent the relationship between input variables (i.e., temperature and mass fraction of the nano-refrigerant) and the observed outputs (i.e., the thermal conductivity and viscosity). Therefore, the GRNN is a reliable tool for making predictions, understanding the system, and informing decision-making for the studied problem.

3.2. The PSO results

Once the GRNN models are obtained, one may use the PSO algorithm to find the optimal solutions. To this end, it is necessary to define decision parameters, and cost function. In this study, the decision parameters are temperature and nano-refrigerant mass fraction. Firstly, the decision parameters are employed to estimate the optimal variables, namely thermal conductivity and viscosity by means of the trained GRNN models. Then, the following cost function is used for the optimization:

$$cost = viscosity/10.51 \; - \; thermalconductivity/0.4 \tag{7}$$

The coefficients of 10.51 mPa.S for the viscosity and 0.4 W/m.K for the thermal conductivity are selected based on the corresponding maximum values in Table 2. The cost function was formulated to balance the competing objectives of maximizing thermal conductivity while minimizing viscosity, as these properties respectively govern heat transfer efficiency and pumping power in refrigeration systems. Both terms were normalized by their maximum experimental values to ensure equal weighting, yielding the dimensionless expression. The negative sign for thermal conductivity explicitly encodes the maximization objective, while positive viscosity reflects minimization. This

normalized formulation creates a Pareto-optimal trade-off surface, where lower cost values indicate superior thermophysical performance. The approach avoids arbitrary weighting factors and directly correlates with system efficiency metrics, as evidenced by the optimal solution achieving both high thermal conductivity and moderate viscosity at minimal cost.

It is assumed that the temperature and nano-refrigerant mass fraction are within the examined range of Table 2. Therefore, in any candidate solution, the temperature should be within 10 to 50 °C, and nano-refrigerant mass fraction is between 0 and 0.8 %.

To minimize the cost function, the PSO with the parameters described in Table 5 is utilized.

The convergence of the best cost values obtained iteratively by the PSO algorithm is shown in Fig. 12. As can be seen, the optimal solution is converged after 15 iterations.

The distribution of the particles of the optimal solution throughout the space of the output variables and decision parameters are illustrated in Fig. 13. Also, the minimum cost, the corresponding optimal output variables, and the corresponding optimum decision parameters achieved by the PSO are summarized in Table 6. As can be seen, the optimum decision parameters are the temperature of 50 °C, and the mass fraction of 0.3092 %, which in turn results in the optimal outputs variables of viscosity of 2.183 mPa.S and the thermal conductivity of 0.3997 W/m.K.

The results of this study have direct applicability in the design of advanced cooling systems. By providing a predictive and optimization framework for thermal conductivity and viscosity, the GRNN-PSO approach facilitates the development of tailored non-Newtonian nano-refrigerants for applications such as vapor compression cycles with low-GWP fluids, compact heat exchangers, and thermal management of electronics and batteries. These optimized nanofluids enable improved heat transfer efficiency while maintaining acceptable flow behavior, supporting energy-efficient, low-carbon cooling technologies in HVAC&R systems.

4. Conclusion

The investigation into the rheological properties of non-Newtonian magneto-nano-refrigerant with $CoFe_2O_4$ nanoparticle cluster concentrations, employing a Radial Basis Function Network (RBFN) prediction method, has yielded insightful results. Through the utilization of Generalized Regression Neural Network (GRNN) models, we have achieved a comprehensive understanding of the complex relationship between input variables, such as temperature and nano-refrigerant mass fraction, and observed outputs, including thermal conductivity and viscosity. The outcomes of this study are listed as follow:

- The efficacy of GRNN models underscore in capturing and representing the intricate dynamics inherent in cooling systems. For the trained datasets, the error values are <8 % for the viscosity, and <1.5 % for the thermal conductivity. For non-trained datasets, the model continues to provide accurate predictions.
- The overall concordance between model predictions and empirical observations underscores the utility of GRNN as a dependable tool for prediction, system understanding, and decision support in nano-refrigerant research. Regression values of 0.99 between the actual

Table 5
The PSO parameters.

parameter	value
φ_1	2.05
φ_2,	2.05
k	1
Max. iteration	30
Swarm Size	10

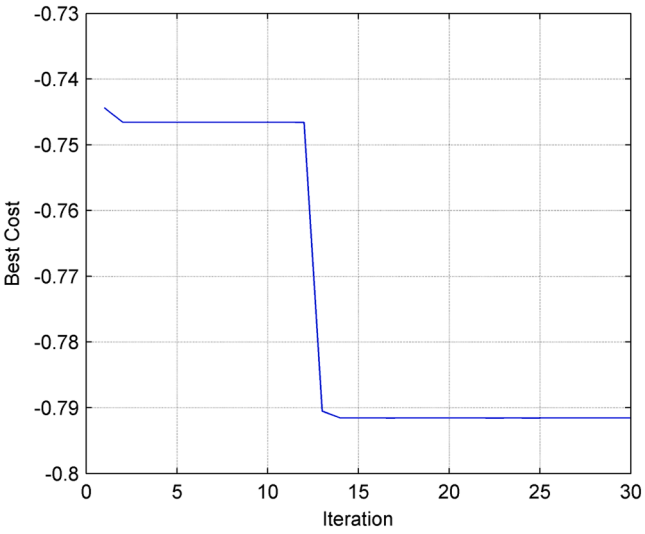

Fig. 12. The convergence of the best cost values.

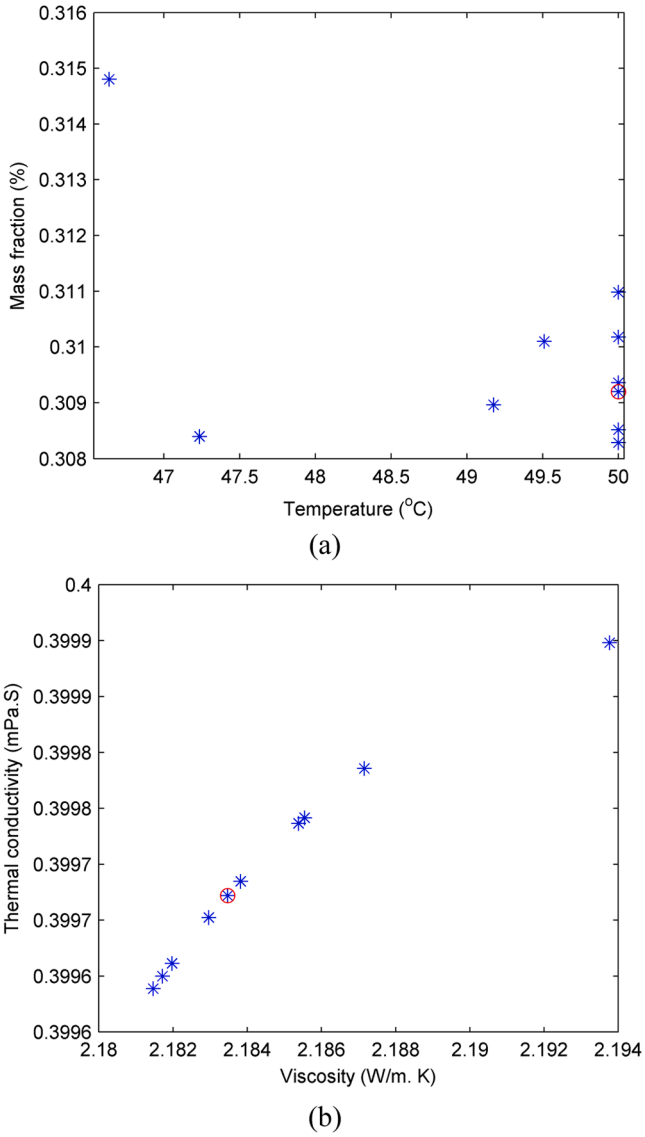

Fig. 13. The distribution of the particles throughout the space of (a) the output variables, and (b) the decision parameters.

Table 6
The PSO results.

The minimum cost	The optimal output variables	The optimum decision parameters
cost = −0.7915	Viscosity = 2.183 mPa.S Thermal conductivity = 0.3997 W/m.K	Temperature = 50 °C Mass fraction = 0.3092 %

output and the model prediction is obtained for both the viscosity and thermal conductivity.

- This study elucidates the effectiveness of employing GRNN models in analyzing and predicting the nonlinear rheological properties of nano-refrigerant, particularly those incorporating $CoFe_2O_4$ nanoparticle clusters. By offering insights into the intricate interplay of variables influencing nano-refrigerant behavior, GRNN facilitates informed decision-making and holds promise for advancing research in this domain.
- The PSO algorithm is employed to find the combination of the thermal conductivity and viscosity. Based on the results, the highest temperature within the examined range of input parameters (i.e., 50 °C) and a moderate nano-refrigerant mass fraction (i.e., 0.3092 %) results in the optimal solution.
- While this study focused on $CoFeO_4$-based nano-refrigerants in an EG-water mixture, the proposed GRNN-PSO framework can be generalized to other materials or base fluids by retraining the model with relevant datasets. The GRNN's architecture is inherently adaptable, and its one-pass learning mechanism allows efficient updates for new systems. Key input parameters may remain broadly applicable, but material-specific properties may require additional experimental data. The optimized nanorefrigerant parameters identified in this study can be applied in real-world refrigeration systems, particularly in vapor compression cycles, compact heat exchangers, and next-generation low-GWP cooling technologies. By reducing thermal resistance while maintaining flow efficiency, these non-Newtonian nanorefrigerants have the potential to enhance heat transfer performance with minimal energy penalty. These insights can support the design of more efficient and environmentally friendly refrigeration systems by guiding the selection and formulation of advanced refrigerants tailored for specific thermal demands. Future work will explore transfer learning and expanded feature spaces to enhance generalizability.

CRediT authorship contribution statement

Mohammad Akbari: Writing – original draft, Visualization, Formal analysis, Data curation. **Seyed Amin Bagherzadeh:** Writing – original draft, Software. **Mohammd Hossein Razavi Dehkordi:** Resources, Data curation. **Alireza Naghsh:** Validation, Formal analysis. **Noushin Azimy:** Writing – review & editing, Software. **Hamidreza Azimy:** Writing – review & editing, Supervision, Project administration, Methodology, Investigation.

Declaration of competing interest

The authors declare that they have no known competing financial interests or personal relationships that could have appeared to influence the work reported in this paper.

References

Abbasian, A.R., Dehkordi, M.H.R., Azimy, N., Azimy, H., Akbari, M., Ayadi, B., Aich, W., Kolsi, L., 2024. Experimental study of preparing the $CoFe_2O_4$ magnetic nanofluid and measuring thermal-fluid characteristics of the stabilized magnetocaloric nanofluid. Mater. Sci. Eng. 306, 117462.

Adogbeji, V.O., Atofarati, E.O., Sharifpur, M., Meyer, J.P., 2025. Experimental investigation and machine learning modeling of the effects of hybridization mixing ratio, nanoparticle type, and temperature on the thermophysical properties of Fe3O4/TiO2, Fe3O4/MgO, and Fe3O4/ZnO-DI water hybrid ferrofluids. J. Therm. Anal. Calorim. 2025/06/14.

Al-Rbaihat, R., Alahmer, H., Alahmer, A., Altork, Y., Al-Manea, A., Awwad, K.Y.E., 2023. Energy and exergy analysis of a subfreezing evaporator environment ammonia-water absorption refrigeration cycle: machine learning and parametric optimization. Int. J. Refrigerat. 154, 182–204, 2023/10/01/.

Alqaed, S., Mustafa, J., Sajadi, S.M., Sharifpur, M., 2024. Enhancing thermal conductivity of water/CeO2-MWCNTs hybrid nanofluid: experimental insights and artificial neural network modeling. J. Therm. Anal. Calorim. 149 (9), 4019–4031, 2024/05/01.

Amani, M., Amani, P., Kasaeian, A., Mahian, O., Wongwises, S., 2017. Thermal conductivity measurement of spinel-type ferrite MnFe2O4 nanofluids in the presence of a uniform magnetic field. J. Mol. Liq. 230, 121–128.

Awua, J.T., Ibrahim, J.S., Krishnan, S.J., Edeoja, A.O., Kuhe, A., Sharifpur, M., Murshed, S.M.S., 2024. Synthesis, characterization, physicochemical, and electrical properties of natural (bio) nanofluids. Environ. Prog. Sustain. Energy. 43 (4), e14397, 2024/07/01.

Azimy, N., Saffarian, M.R., 2023. Investigation of thermal characteristics and entropy generation in a solar collector including Fly Ash-Cu hybrid nanofluids: numerical approach using mixture model. Eng. Anal. Bound Elem. 152, 169–184.

Azimy, H., Azimy, N., Meghdadi Isfahani, A.H., Bagherzadeh, S.A., Farahnakian, M., 2023. Analysis of thermal performance and ultrasonic wave power variation on heat transfer of heat exchanger in the presence of nanofluid using the artificial neural network: experimental study and model fitting. J. Therm. Anal. Calorim. 148 (16), 8009–8023.

Azimy, N., Saffarian, M.R., Noghrehabadi, A., 2024. Thermal performance analysis of a flat-plate solar heater with zigzag-shaped pipe using fly ash-Cu hybrid nanofluid: CFD approach. Environment. Sci. Pollut. Res. 31 (12), 18100–18118.

Borode, A., Tshephe, T., Olubambi, P., Sharifpur, M., Meyer, J., 2023. Experimental study and ANFIS modelling of the thermophysical properties and efficacy of GNP-Al2O3 hybrid nanofluids of different concentrations and temperatures. SN Appl. Sci. 5 (12), 337, 2023/11/15.

Borode, A., Tshephe, T., Olubambi, P., Sharifpur, M., Meyer, J., 2024. Effects of temperature and nanoparticle mixing ratio on the thermophysical properties of GNP–Fe2O3 hybrid nanofluids: an experimental study with RSM and ANN modeling. J. Therm. Anal. Calorim. 149 (10), 5059–5083, 2024/05/01.

Chu, Y.-M., Ibrahim, M., Saeed, T., Berrouk, A.S., Algehyne, E.A., Kalbasi, R., 2021. Examining rheological behavior of MWCNT-TiO2/5W40 hybrid nanofluid based on experiments and RSM/ANN modeling. J. Mol. Liq. 333, 115969.

Dehkordi, M.H.R., Alizadeh, A.a., Zekri, H., Rasti, E., Kholoud, M.J., Abdollahi, A., Azimy, H., 2023. Experimental study of thermal conductivity coefficient of GNSs-WO3/LP107160 hybrid nanofluid and development of a practical ANN modeling for estimating thermal conductivity. Heliyon 9 (6).

DENG, Miaosen, HU, Chunyan, SUN, Jiaxian, et al., 2024. Low temperature heating design and its optimization of low cost aeroengine controller. J. Ordna. Equip. Eng. 45 (2), 46–53, 143.

El Jery, A., Satishkumar, P., Salman, H.M., Khedher, K.M., 2023a. Comparison of different approaches for numerical modeling of nanofluid subcooled flow boiling and proposing predictive models using artificial neural network. Progr. Nuclear Energy. 156, 104540.

El Jery, A., Ramírez-Coronel, A.A., Gavilán, J.C.O., Al-Ansari, N., Sammen, S.S., 2023b. Proposing empirical correlations and optimization of Nu and Sgen of nanofluids in channels and predicting them using artificial neural network. Case Stud. Therm. Eng. 45, 102970.

Esfe, M.H., Bahiraei, M., Hajmohammad, M.H., Afrand, M., 2017. Rheological characteristics of MgO/oil nanolubricants: experimental study and neural network modeling. Int. Communicat. Heat Mass Trans. 86, 245–252.

Esfe, M.H., Amoozadkhalili, F., Toghraie, D., 2023. Determining the optimal structure for accurate estimation of the dynamic viscosity of oil-based hybrid nanofluid containing MgO and MWCNTs nanoparticles using multilayer perceptron neural networks with Levenberg-Marquardt Algorithm. Powder Technol. 415, 118085.

Eshgarf, H., Nadooshan, A.A., Raisi, A., Afrand, M., 2023. Experimental examination of the properties of Fe_3O_4/water nanofluid, and an estimation of a correlation using an artificial neural network. J. Mol. Liq. 374, 121150.

GAO, Peng, WANG, Rui, YANG, Shuifeng, et al., 2024. Research on rapid evaluation method for ventilation and cooling in engine cabin. J. Ordn. Equip. Eng. 45 (5), 188–195, 230.

Hasan, M.M., Rahman, M.M., Abu Bakar, S., Kabir, M.N., Ramasamy, D., Saifullah Sadi, A.H.M., 2025. Performance evaluation of various training functions using ANN to predict the thermal conductivity of EG/water-based GNP/CNC hybrid nanofluid for heat transfer application. J. Therm. Anal. Calorim. 150 (3), 1907–1932, 2025/02/01.

Hatamleh, R.I., Rawa, M.J., Abu-Hamdeh, N.H., Shboul, B., Karimipour, A., 2023. Simulation of nanofluid flow in a solar panel cooling system to investigate the panel's electrical-thermal efficiency with artificial neural network. J. Taiwan Inst. Chemic. Eng. 148, 104879.

Hemmat Esfe, M., Hosseini Tamrabad, S.Naser, Toghraie, D., Hatami, H., 2024. Presenting the best correlation relationship for predicting the dynamic viscosity of CuO nanoparticles in ethylene glycol -water base fluid using response surface methodology. Arab. J. Chem. 17 (1), 105467, 2024/01/01/.

Kamsuwan, C., Wang, X., Piumsomboon, P., Pratumwal, Y., Otarawanna, S., Chalermsinsuwan, B., 2023. Artificial neural network prediction models for nanofluid properties and their applications with heat exchanger design and rating simulation. Int. J. Therm. Sci. 184, 107995.

Karakaş, A., Harikrishnan, S., Öztop, H.F., 2022. Preparation of EG/water mixture-based nanofluids using metal-oxide nanocomposite and measurement of their thermophysical properties. Therm. Sci. Eng. Prog. 36, 101538, 2022/12/01/.
Khosravi, R., Zamaemifard, M., Safarzadeh, S., Passandideh-Fard, M., Teymourtash, A.R., Shahsavar, A., 2023. Predicting entropy generation of a hybrid nanofluid in microchannel heat sink with porous fins integrated with high concentration photovoltaic module using artificial neural networks. Eng. Anal. Bound Elem. 150, 259–271.
Kim, D., Liu, H., Yang, X., Yang, F., Morfitt, J., Arami-Niya, A., Ryu, M., Duan, Y., May, E. F., 2021. Thermal conductivity measurements and correlations of pure R1243zf and binary mixtures of R32 + R1243zf and R32 + R1234yf. Int. J. Refrigerat. 131, 990–999, 2021/11/01/.
Kumar, D., Kumar, A., Subudhi, S., 2023. Thermal behavior of magnetite nanofluid under magnetic field: an experimental study and development of predictive model to predict thermal conductivity. J. Eng. Thermophys. 32 (1), 100–116.
Li, Y., Xia, Y., Deng, W., Gao, X., Li, H., Gao, X., 2025. Nucleate boiling heat transfer and critical heat flux in controllable droplet trains cooling. Appl. Therm. Eng. 267, 125824.
Mandal, D.K., Biswas, N., Manna, N.K., Gayen, D.K., Gorla, R.S.R., Chamkha, A.J., 2022. Thermo-fluidic transport process in a novel M-shaped cavity packed with non-darcian porous medium and hybrid nanofluid: application of artificial neural network (ANN). Phys. Fluid. 34 (3).
Melaibari, A.A., Khetib, Y., Alanazi, A.K., Sajadi, S.M., Sharifpur, M., Cheraghian, G., 2021. Applying artificial neural network and response surface method to forecast the rheological behavior of hybrid nano-antifreeze containing graphene oxide and copper oxide nanomaterials. Sustainability 13 (20), 11505.
Momin, M., Nwaokocha, C.N., Sharifpur, M., Cheraghian, G., Meyer, J.P., El-Rahman, M. A., 2025. Investigation of thermal and electrical properties of ternary composite nanofluids using MgO, ZnO, and MWCNT nanoparticles. Resul. Phys. 70, 108139, 2025/03/01/.
Mondal, D., Hori, Y., Kariya, K., Miyara, A., Alam, M.Jahangir, 2020. Measurement of viscosity of a binary mixture of R1123 + R32 refrigerant by tandem capillary tube method. Int. J. Thermophys. 41 (6), 83, 2020/04/11.
Mondal, D., Kariya, K., Tuhin, A.R., Miyoshi, K., Miyara, A., 2021. Thermal conductivity measurement and correlation at saturation condition of HFO refrigerant trans-1,1,1,4,4,4-hexafluoro-2-butene (R1336mzz(E)). Int. J. Refrigerat. 129, 109–117, 2021/09/01/.
Mondal, D., Kariya, K., Tuhin, A.R., Amakusa, N., Miyara, A., 2022a. Viscosity measurement for trans-1,1,1,4,4,4-hexafluoro-2-butene (R1336mzz(E)) in liquid and vapor phases. Int. J. Refrigerat. 133, 267–275, 2022/01/01/.
Mondal, D., Tuhin, A.R., Kariya, K., Miyara, A., 2022b. Measurement of kinematic viscosity and thermal conductivity of 3,3,4,4,5,5-HFCPE in liquid and vapor phases. Int. J. Refrigerat. 140, 150–165, 2022/08/01/.
Noghrehabadi, A., Hajidavalloo, E., Moravej, M., 2016. Experimental investigation of efficiency of square flat-plate solar collector using SiO2/water nanofluid. Case Stud. Therm. Eng. 8, 378–386.
Pierantozzi, M., Tomassetti, S., Di Nicola, G., 2023. Modeling liquid thermal conductivity of low-GWP refrigerants using neural networks. Appl. Sci. 13.].
Pourpasha, H., Farshad, P., Heris, S.Z., 2021. Modeling and optimization the effective parameters of nanofluid heat transfer performance using artificial neural network and genetic algorithm method. Energy Report. 7, 8447–8464.
Pourrajab, R., Noghrehabadi, A., Hajidavalloo, E., Behbahani, M., 2020. Investigation of thermal conductivity of a new hybrid nanofluids based on mesoporous silica modified with copper nanoparticles: synthesis, characterization and experimental study. J. Mol. Liq. 300, 112337.
Pourrajab, R., Noghrehabadi, A., Behbahani, M., Hajidavalloo, E., 2021. An efficient enhancement in thermal conductivity of water-based hybrid nanofluid containing MWCNTs-COOH and Ag nanoparticles: experimental study. J. Therm. Anal. Calorim. 143, 3331–3343.
Puspitasari, P., Permanasari, A.A., Wahyudi, B., Pramono, D.D., Hastuty, S., 2025. Investigation of physicochemical and magnetic properties of zinc ferrite (ZnFe2O4) with different ultrasonic power for enhancement of thermal conductivity of refrigeration oils. Mater. Res. Proceed. 53.
Qun, Z.H.A.N.G., Xiaobiao, S.H.A.N.G., Wenbo, W.A.N.G., et al., 2024. Heat dissipation performance of lithium battery at high temperature based on CPCM liquid cooling fin coupling. J. Ordn. Equip. Eng. 45 (4), 82–89.
Ramadhan, A.I., Diniardi, E., Basri, H., Almanda, D., Azmi, W.H., 2023. Experimental investigation of thermal conductivity of Al2O3-TiO2-SiO2 nanofluids in EG/water mixture for automotive radiator cooling system. AIP Conf. Proc. 2706 (1), 020007.
Ru, Y., Ali, A.B.M., Qader, K.H., Abdulaali, H.K., Jhala, R., Ismailov, S., Salahshour, S., Mokhtarian, A., 2025. Accurate prediction of the rheological behavior of MWCNT-Al2O3/water-ethylene glycol nanofluid with metaheuristic-optimized machine learning models. Int. J. Therm. Sci. 211, 109691, 2025/05/01/.
Ruhani, B., Barnoon, P., Toghraie, D., 2019. Statistical investigation for developing a new model for rheological behavior of Silica–ethylene glycol/water hybrid newtonian nanofluid using experimental data. Physica A. 525, 616–627.
Safaei, M.R., Hajizadeh, A., Afrand, M., Qi, C., Yarmand, H., Zulkifli, N.W.B.M., 2019. Evaluating the effect of temperature and concentration on the thermal conductivity of ZnO-TiO2/EG hybrid nanofluid using artificial neural network and curve fitting on experimental data. Physica A. 519, 209–216.
Salins, S.S., Kumar, S., Ganesha, A., Reddy, S.K., 2024. Machine learning-based optimization and performance analysis of cooling towers. J. Build. Engineering 96, 110415.
Seawram, S., Nimmanterdwong, P., Sema, T., Piemjaiswang, R., Chalermsinsuwan, B., 2022. Specific heat capacity prediction of hybrid nanofluid using artificial neural network and its heat transfer application. Energy Report. 8, 8–15.
Sepehrnia, M., Maleki, H., Behbahani, M.F., 2023. Tribological and rheological properties of novel MoO3-GO-MWCNTs/5W30 ternary hybrid nanolubricant: experimental measurement, development of practical correlation, and artificial intelligence modeling. Powder Technol 421, 118389.
Sepehrnia, M., Mohammadzadeh, K., Rozbahani, M.H., Ghiasi, M.J., Amani, M., 2024. Experimental study, prediction modeling, sensitivity analysis, and optimization of rheological behavior and dynamic viscosity of 5W30 engine oil based SiO2/MWCNT hybrid nanofluid. Ain Shams Eng. J. 15 (1), 102257.
Shoaib, M., Sabir, M.T., Raja, M.A.Z., Khan, M.A.R., Nisar, K.S., 2023. Intelligent computing for unsteady flow of a hybrid nanofluid over a stretching/shrinking surface: an application of artificial neural networks. Waves Random Complex Media. 1–18.
Sun, Y., Wang, J., Wang, X., He, M., Hu, Y., 2021. An experimental investigation and correlation of the viscosity refrigerant/oil solutions. Int. J. Refrigerat. 121, 152–158, 2021/01/01/.
Tran, D.X., Tuhin, A.R., Morshed, M., Hirata, R., Miyara, A., 2025. Measurement and empirical model of viscosity of the novel refrigerant R-1132(E). Int. J. Thermophys. 46 (5), 65, 2025/03/13.
Vaferi, B., Samimi, F., Pakgohar, E., Mowla, D., 2014. Artificial neural network approach for prediction of thermal behavior of nanofluids flowing through circular tubes. Powder Technol. 267, 1–10.
Wen, T., Zhu, G., Jiao, K., Lu, L., 2021. Experimental study on the thermal and flow characteristics of ZnO/water nanofluid in mini-channels integrated with GA-optimized ANN prediction and CFD simulation. Int. J. Heat Mass Transf. 178, 121617.
Yan, S.-R., Kalbasi, R., Nguyen, Q., Karimipour, A., 2020. Rheological behavior of hybrid MWCNTs-TiO2/EG nanofluid: a comprehensive modeling and experimental study. J. Mol. Liq. 308, 113058.
Yasmin, H., Giwa, S.O., Noor, S., Sharifpur, M., 2023. Thermal conductivity enhancement of metal oxide nanofluids: a critical review. Nanomaterials 13.].
Ünvar, S., Çolak, A.B., Menlik, T., 2023. Experimental analysis of the effect of nanofluid use on power and efficiency enhancement in heat pipe solar collectors and modeling using artificial neural networks. Heat Transf. Res. 54 (13).